Characteristics of Intense Wind in Mountain Area Based on Field Measurement: Focusing on Thunderstorm Winds

Guoqing Huang, Yan Jiang, Liuliu Peng, Giovanni Solari, Haili Liao, Mingshui Li

Guoqing Huang, Professor,
School of Civil Engineering, Chongqing University, Chongqing, 400044, China;
School of Civil Engineering, Southwest Jiaotong University, Chengdu, 610031, China,
Email: ghuang1001@gmail.com

Yan Jiang, PhD student,
School of Civil Engineering, Southwest Jiaotong University, Chengdu, 610031, China,
Email: xnjtjiangyan@163.com

Liuliu Peng (Corresponding author), Postdoctor,
School of Civil Engineering, Chongqing University, Chongqing, 400044, China,
Email: liuliu.peng@cqu.edu.cn

Giovanni Solari, Professor,
Department of Civil, Chemical and Environmental Engineering, University of Genoa, Via Montallegro, 1, 16145 Genoa, Italy
Email: giovanni.solari@unige.it

Haili Liao, Professor,
School of Civil Engineering, Southwest Jiaotong University, Chengdu, 610031, China,
Email: hlliao@swjtu.edu.cn

Mingshui Li, Professor,
School of Civil Engineering, Southwest Jiaotong University, Chengdu, 610031, China,
Email: lms_rcwe@126.com

ABSTRACT

With the development of mountain areas, more wind-sensitive infrastructures are constructed. In the design of these infrastructures, the wind loading cannot be accurately obtained from the code based on the flat area. Hence, it is of great importance to study the mountain wind characteristics. In this study, the wind field measurement was initiated in a mountain area of western China. After the examination of the measured data, two typical wind events including the thunderstorm wind and thermally developed wind are highlighted. To extract and separate these wind events, an automatic classification method is proposed. The thunderstorm wind is analyzed in order to capture the rapid variation of its maximum wind speed, mean temperature and mean humidity through the boxplot method while the analysis of thermally developed winds relies on the correlation between the mean wind speed and mean temperature. Since the thunderstorm wind is relatively more important for wind engineering, its wind characteristic is focused hereafter and analyzed in detail based on the ultrasonic anemometer data. The characteristics of the thermally developed wind and other wind will be the matter of further studies and investigations. Results show that the characteristics of the thunderstorm wind measured in the mountainous area have no relevant difference in comparison with those in the flat area. Due to the limited data, the above results deserve further investigations when more measurements will become available.

Keywords: Field measurement; Mountain terrain; Wind characteristics; Wind classification; Thunderstorm wind; Thermally developed wind

1 Introduction

With the development of mountain areas, more and more infrastructures such as long-span bridges, transmission lines and wind farms are constructed or to be constructed. This is particularly obvious for China because two third of the territory of this world's second largest economy belongs to the mountain area. Typical projects include Hunan Aizhai Bridge, Sichuan-Anhui 1000 kV ultra-high transmission line and Yunnan Daguashan wind farm. These infrastructures are wind-sensitive and their designs are usually controlled by the wind loading. To determine the design wind loading, the study of wind characteristics is a precondition. In the mountain area, the wind will accelerate when the wind flows along the valley due to the channel effect while the separation and speed-up effect usually occurs if the wind flows over the valley or hill (Taylor and Teunissen, 1987; Salmon et al. 1988; Berg et al. 2011; Li et al. 2017). More importantly, the mountain environment tends to create a mixed wind climate due to the complex terrain and meteorological condition (Chow et al. 2013). Therefore, the wind and its distribution in mountain terrains are obviously different from or may be larger than those in the homogeneous terrain such as the plain and coastal areas.

Because the wind loading for these infrastructures in mountain terrains cannot be accurately obtained from the design code, which is derived from the homogeneous terrain (Castino et al. 2003; Chock and Cochran, 2005), various approaches including the theoretical modeling (Jackson and Hunt, 1975; Hunt et al. 1988), numerical simulation (Cao et al. 2012; Burlando et al. 2013; Cantelli et al. 2017; Huang et al. 2018), wind tunnel test (Li et al. 2010; Li et al. 2017) and field measurement (Carrera et al. 2009; Huang et al. 2015, Fenerci et al. 2017; Fenerci and Øiseth, 2018) are used. Although the field measurement has the disadvantages such as limited points, high cost and non-repeatability, it can provide the first-hand information for the wind in mountain terrains. Scholars in the field of meteorology have investigated the wind characteristics in the mountain terrain since 1950s. Defant (1951) provided a classic explanation of the daily thermally developed wind based on the field measurement at the Alps. Davidson (1963) used balloons to study wind characteristics of the leeward in a ridge and the variation of the wind profile. Whiteman (1990) discussed the concept of the terrain magnification factor, atmospheric heat balance and the evolution of thermally developed winds using the field measurement in mountain terrains. Jackson et al. (2013) carried out a detailed review and analysis of wind characteristics such as the mountain breeze, dorsal mountain wind and valley wind. In summary, these studies mainly focus on the mean wind characteristics and less attention is paid on the fluctuation. In addition, the strong wind is usually not highlighted by the field measurement in the meteorological community.

Compared with the meteorological community, the wind field measurement in the mountain terrain is relatively limited from the perspective of the wind engineering. Mitsuta et al. (1983) carried out a large-scale study on the wind field along the transmission line, focusing on the variation of the average wind profile and the wind fluctuation characteristics along the ridge line in the mountain area. Momomura et al. (1997) and Okamura et al. (2003) installed an ultrasonic anemometer on the transmission tower to analyze the mean wind speed, turbulence intensity and turbulence integral scale at the measured site. Zhu et al. (2011) carried out the field observation on the wind profile of the deep valley at the bridge site of Baling River Bridge by the radar wind profiler. Fenerci et al. (2017) and Fenerci and Øiseth (2018) analyzed and discussed the results of a wind monitoring campaign at the complex orography site of the Hardanger Bridge, Norway. Burlando et al. (2017a) investigated the characteristics of downslope winds in the Liguria Region using an anemometric monitoring network with 15 ultrasonic anemometers and 2 LiDARs. Their emphases are mainly placed on the vertical wind profile, turbulence intensity and gust factor. In these limited literatures, less attention was paid on the mixed wind climate in mountain terrains through field measurement, which has been discussed in the flat and coastal area (Lombardo et al. 2009; De Gaetano et al. 2014; Zhang et al. 2018a). In addition, the wind fluctuation characteristics in mountain terrains are also relatively less reported.

In this paper, the mountain wind characteristics based on the field measurement are focused. First of all (Section 2), the field observation at a bridge site in southwest China is briefly introduced. Then (Section 3), the measured wind events are classified into different categories based on the proposed automatic classification method. Furthermore (Section 4), the wind characteristics of the thunderstorm wind are analyzed in detail using the ultrasonic anemometer data measured in the mountain area. Lastly (Section 5), some observations and conclusions are summarized.

2 Wind field measurement

The wind field measurement was initiated by the construction of Puli Bridge in Yunnan, a southwest province in China. Puli Bridge is a suspension bridge with a main span of 628 m. At the top of an unobstructed hill close to the bridge, an observation tower was erected for measuring winds, as shown in Fig. 1(a). The altitude of the base of the observation tower is 1890 m. At the northeast, southwest and southeast of the observational tower, there are three major hills with the approximately same altitude of 2100 m. These hills form a “Y” shape valley with a lowest altitude of 1360 m. The details can be found in Fig. 1(b). The mountain area of interest is mainly covered by small trees. Near the observational tower, there are three meteorological stations, namely, Xuanwei, Weining and Panxian, as shown in Fig. 1(c). Their distances with the observation tower are about 52, 67 and 70 km, respectively. The annual daily average wind speed and precipitation of these stations based on the 30-year data from 1981 to 2010 are shown in Fig. 2. It can be seen that the strong wind usually occurs on February and March while the wind speed in summer is relatively small. In addition, the precipitation in summer is significantly greater than that in other seasons. This is maybe related to the thunderstorm happened in summer.

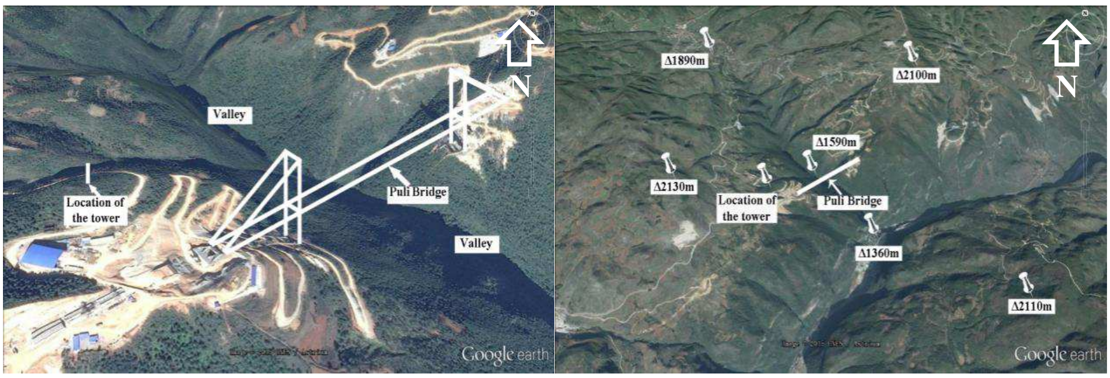

(a) Location of observation tower (b) Surrounding topography

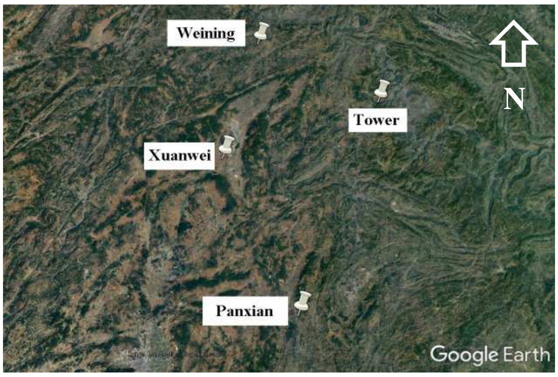

(c) Nearby meteorological station

Fig. 1 Key information related to the observation tower (Based on Google Earth)

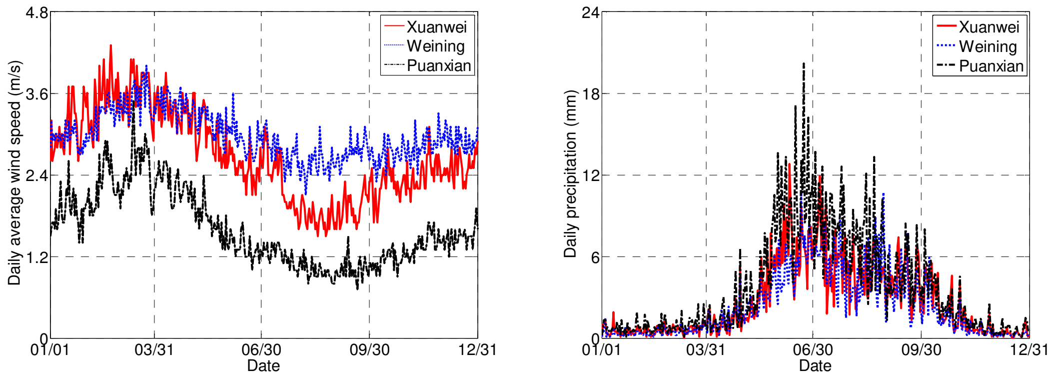

(a) Annual daily average wind speed (b) Annual daily precipitation

Fig. 2 Annual daily average wind speed and precipitation (1981-2010)

The layout of the measurement instrument on the observation tower and the corresponding key parameters are shown in Fig. 2 and Table 1, respectively. It can be seen that five cup anemometers, whose distance constant is 3 m, had been mounted at interval of 10 m from the height of 10 m. Meanwhile, three wind direction vanes were installed at the height of 10, 30 and 50 m, respectively. In addition to the cup anemometers and wind direction vanes, some other measurement instruments were also installed to measure the temperature, relative humidity and barometric pressure. These instruments are all located on an 8-m high platform. It should be noted that the brand of these aforementioned measurement instruments is NRG which belongs to the company Wind & Sun. The sampling frequency of these NRG measurement instruments is 1 Hz. The mean value, maximum value, minimum value and standard deviation of the wind speed, wind direction, temperature, relative humidity and barometric pressure on 10-min interval are stored by NRG measurement instruments, as shown in Table 1.

In order to measure the wind fluctuation, two three-dimensional (3D) ultrasonic anemometers, whose model is Young 81000, were also installed at the height of 30 and 50 m of the tower, as shown in Fig. 3 and Table 1. The ultrasonic anemometer has two formats of data acquisition, i.e., three-component wind speeds and the instantaneous 3D wind speed, direction and elevation. In our measurement, the latter is adopted and stored which also can be easily converted to the three-component wind speeds. The sampling frequency is set to 4 Hz. Note that the data at the first 9 months were obtained by the wire method while they were acquired by wireless instrumentation system for the other time (Huang et al. 2015).

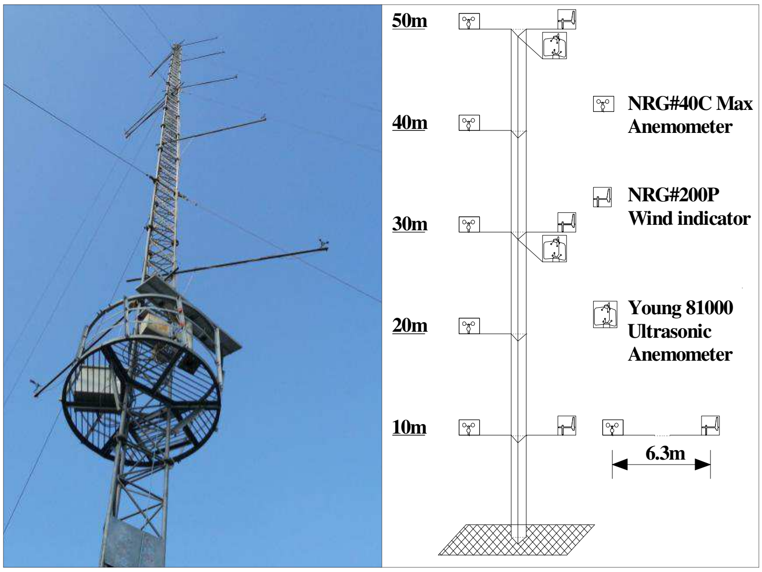

Fig. 3 Layout of the measurement instruments

Table 1 Summary of measurement instrument parameters

Instrument model	Instrument type	Height (m)	Frequency (Hz)	Stored data
NRG #40C	3-cup anemometer	10/20/30/40/50	1	The mean value, maximum value, minimum value and standard deviation of the horizontal wind speed, wind direction, temperature, relative humidity and barometric pressure based on 10-min interval
NRG #200P	Continuous rotation potentiometric wind direction vane	10/30/50	1	
NRG #110S	Integrated circuit temperature sensor with six plate radiation shield	8	1	
NRG #RH5X	Polymer resistor humidity sensor	8	1	
NRG #BP20	Micromachined integrated circuit absolute pressure sensor	8	1	
Young 81000	Three-dimensional (3D) ultrasonic anemometer	30/50	4	Instantaneous 3D wind speed, direction and elevation

The observation lasted over 980 days, from Feb 9, 2013 to Oct 16, 2015. During this period, the 956-day valid data measured from the cup anemometers were obtained while those measured by the ultrasonic anemometers were relatively less due to wireless transmission problems. Therefore, the former will be adopted in the following wind data classification. Based on the classification result, the final data set from the ultrasonic anemometers will be selected to analyze wind characteristics.

3 Wind data classification

As mentioned previously, the mountain environment tends to create a mixed wind climate due to the complex terrain and meteorological condition. In our measurement, it is confirmed by the examination of the measured data. Before analyzing the mixed wind climate, the classification of wind events is required. This treatment has two major advantages. First, the extreme wind speed can be estimated more accurately. Second, the distinct statistical models used for modeling each phenomenon are more suitable to describe their homogeneous characteristics (Gomes and Vickery, 1977/1978; Cook et al. 2003; Zhang et al. 2018a).

Currently, there are two types of methods used for data extraction and classification (De Gaetano et al. 2014). The first type identifies the wind event from the prospective of atmospheric sciences, providing detailed investigations of the weather scenario in which a single event occurs (e.g., Gunter and Schroeder, 2013). This approach, which is beyond the scope of this paper, is maybe unsuitable with regard to the analyses of extensive datasets of measurements as usually happens in wind engineering evaluations. The second, used herein, is just based on the prospective of wind engineering (e.g., Choi and Tanurdjaja, 2002; Lombardo et al. 2009). In the latter, a preliminary, rapid and automatic extraction and classification is often carried out directly based on the data with 10-min interval. In many cases, a detailed investigation of single event of particular interest follows a preliminary extraction and separation of the second type (Burlando et al. 2017b).

In this study, each daily wind time history is assumed to be independent. The reason for such an assumption will be explained in the next section. The wind classification is performed through the examination of the daily variation of the 10-min statistical parameter. Since the attention is mainly placed on the characteristics of intense winds, the intense wind event with the daily largest 10-min mean wind speed greater than a threshold is chosen. Currently, there are differences about the selection of the threshold wind speed of intense winds. Researchers have used the following 10-min mean wind speeds as the thresholds: 5 m/s (Masters et al. 2010; Shu et al. 2015), 8 m/s (Vega, 2008) and 10 m/s (Shu et al. 2015; Solari et al. 2015). In this study, the 10-min threshold mean wind speed is set to 8 m/s. Among the 956-days wind events, there exist 90 days satisfying the selection criterion. In the following, the typical wind event in the mountain area will be introduced first (Section 3.1). Then (Section 3.2), an automatic classification method is proposed. At the last (section 3.3), the classification results and discussions are given.

3.1 Typical wind events

Based on the examination of the measured data, two typical wind events have been found in the mountain terrain:

(1) Thunderstorm wind. The main features of the thunderstorm wind are dramatic change and short duration. These can be reflected by the maximum wind speed, mean wind direction, mean temperature and mean humidity on 10-min interval. Note that the term "maximum wind speed" used in this paper is the maximum value of the 1-s sampled wind speed observed over the 10-min period, as shown in Table 1. A typical thunderstorm wind event can be characterized by a sudden increase in the maximum wind speed, a sudden change in the mean wind direction, a rapid drop of the mean temperature and a sharp increase of the mean humidity, as shown in Fig. 4. It can be seen that these parameters have noteworthy variations during the occurrence of the thunderstorm wind. For instance, the maximum wind speed at 10 m height increases from 5 m/s to 23 m/s; the mean wind direction varies from 40 ° to 270 °;

the mean temperature decreases from 24 °C to about 19 °C; the mean humidity increases from 78% to about 95%. The similar variation trends for these parameters have also been reported in literature (e.g., Choi and Hidayat, 2002; Choi, 2004).

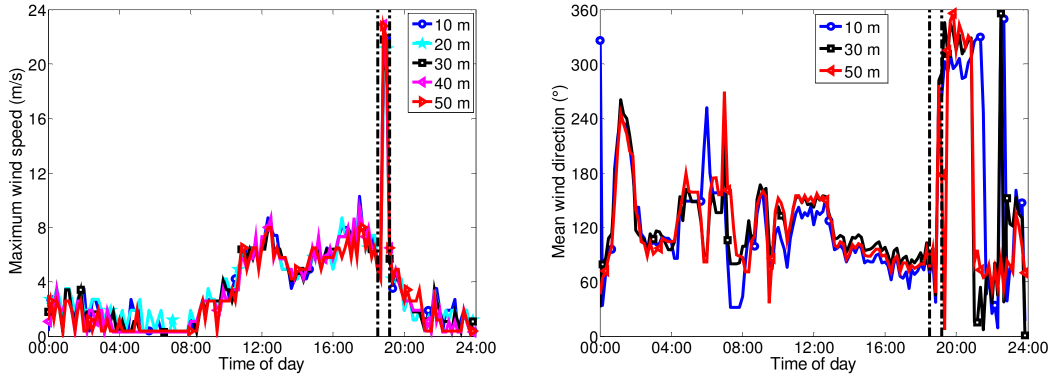

(a) Maximum wind speed (b) Mean wind direction

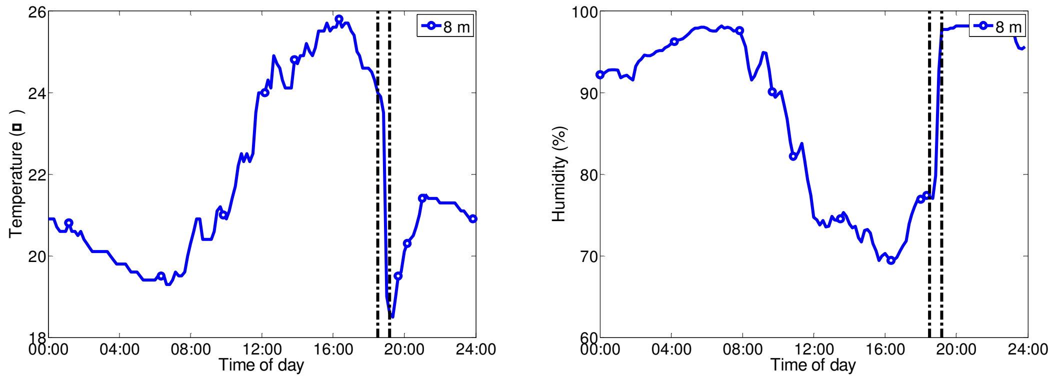

(c) Mean temperature (d) Mean humidity

Fig. 4 A typical thunderstorm wind event (08/08/2014)

(2) Thermally developed wind. This wind event is fundamentally driven by the temperature gradient between the mountain slope and valley (Chow et al. 2013). Therefore, its daily variation trend of the 10-min mean wind speed has strong correlation with that of the temperature. Specifically, the wind speed in the morning generally reaches the lowest level of the whole day. With the rise of the sun, the temperature gradually increases. Correspondingly, the mean wind speed increases slowly. After arriving at a suitable threshold, the wind speed begins to increase rapidly and reaches its maximum at around 16:00. Then, the wind speed begins to decrease due to the temperature drop. At the last, the wind speed returns to the lowest speed level (Defant 1951; Whiteman 1990). A typical thermally developed wind event is illustrated in Fig. 5. It can be seen that the mean wind speed and temperature have high positive correlation while the mean wind speed and humidity exhibit negative correlation.

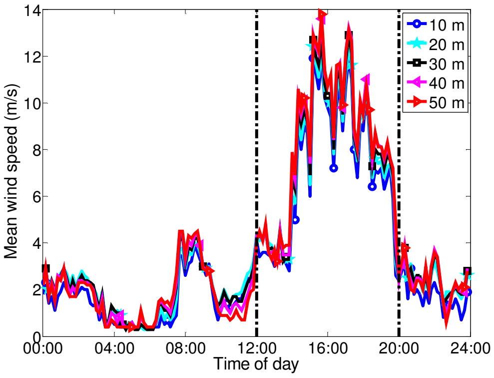

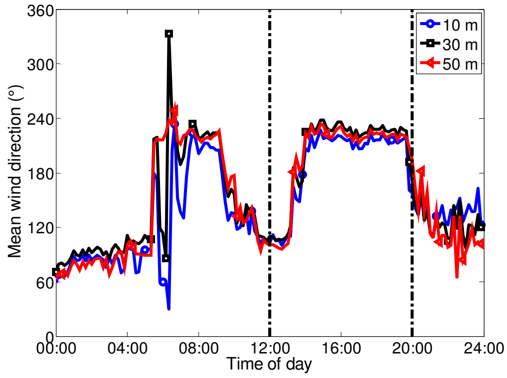

(a) Mean wind speed (b) Mean wind direction

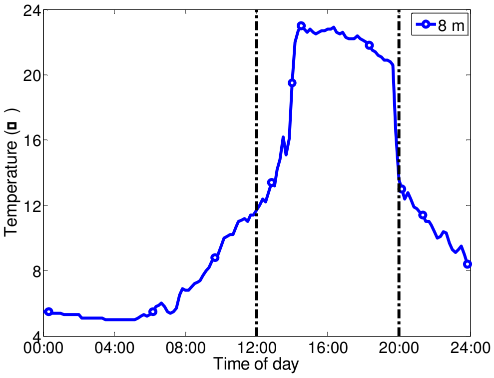

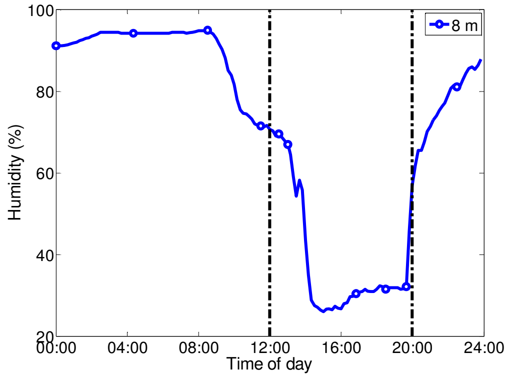

(c) Mean temperature (d) Mean humidity

Fig. 5 A typical thermally developed wind event (03/05/2014)

Once the wind event cannot match the characteristics of the above two typical wind events, it will be classified into "Other wind" which is maybe caused by the large-scale atmospheric depression. For sake of simplicity, the aforementioned three wind events, i.e., thunderstorm wind, thermally developed wind and other wind are referred to as TW, TDW and OW, respectively.

From preceding discussions, it can be observed that the two most typical wind events, namely the thunderstorm wind and the thermally developed wind, generally occur during one day. Hence, the assumption of independent daily wind event is appropriate. For other winds, in particular the large-scale atmospheric depression, this assumption may be not appropriate since their durations may be larger than one day. Nonetheless, focusing on thunderstorm and thermally developed wind, this is not very important. Based on this assumption, the classification of the wind events is conducted, which will be introduced in the next section.

3.2 Automatic classification for winds

The 90 most intense (daily) wind events can be separated into the aforementioned three categories through an automatic classification method which includes two following steps. First, the thunderstorm wind will be extracted by a proposed separation algorithm 1. Then, the remaining wind events will be classified into the thermally developed wind or other wind based on whether they could pass a proposed separation algorithm 2. It is worth noting that if a daily wind event simultaneously passes the separation algorithms 1 and 2, it will be treated as a thunderstorm wind event.

3.2.1 Separation algorithm for thunderstorm winds

Currently, the separation and identification methods of thunderstorm winds from the prospective of wind engineering can be mainly framed into two families. The first family relies on the record of the thunderstorm or its relevant meteorological information, e.g., thunder, lighting, rainfall and abrupt temperature drop (Riera and Nanni, 1989; Choi and Hidayat, 2002; Lombardo et al. 2009). This family of separation methods is very direct. Nonetheless, the meteorological information such as the thunder, lighting and rainfall are sometimes limited for the wind engineering. The second family identifies the thunderstorm wind based on the mean wind speed, maximum wind speed and their derived information such as the gust factor (Kasperski, 2002; Durañona et al. 2007; De Gaetano et al. 2014). This family of separation methods requires relatively less raw information. Nonetheless, the selection of the separation criterion for the derived information is difficult since it may depend on the meteorological and topographical conditions. For example, the reference gust factor used in De Gaetano et al (2014) was calibrated based on the flat port area. It may not be used in the separation of thunderstorm winds in the mountain area. To alleviate these difficulties, a new automatic separation algorithm with more flexibility is proposed from the perspective of the wind engineering.

Generally, the parameters such as the maximum wind speed, mean wind direction, mean temperature and mean humidity will have rapid variation when the thunderstorm occurs (Choi, 2004). Among them, the rapid variation of the mean wind direction is difficult to be quantified in comparison with that of other parameters. In addition, the variation is not always apparent. For example, certain positions of the thunderstorm downdraft with respect to the anemometer may not cause a clear variation of the mean wind direction. Moreover, the variation of the wind direction is often so rapid that its 10-min mean value cannot capture this phenomenon. Thus, it will not be used in the proposed algorithm. For the maximum wind speed, the rapid increase and decrease forms a peak, as shown in Fig. 6(a). The value of this peak may be large especially in the case of microbursts. Besides, the difference between two neighboring values of the mean temperature and mean humidity generally exhibit an abrupt decrease and increase, forming peaks/valleys at the occurrence instant of the thunderstorm wind, as shown in Fig. 6(b) and 6(c), respectively. These peaks/valleys may be treated as outliers from the prospective of statistics. In addition, the occurrence instants of these outliers should be very close due to the fact that they are caused by the same thunderstorm event.

Currently, there are many methods of identifying outliers such as 3σ method and boxplot method. In this study, the boxplot method is chosen and the details are provided in Appendix A. The boxplot of the parameter for a typical thunderstorm wind is shown in Fig. 6. It can be seen that the outliers have been found in all the parameters, and the largest outlier of the maximum wind speed is 22.8 m/s. In addition, the occurrence instants of the outliers are almost simultaneous.

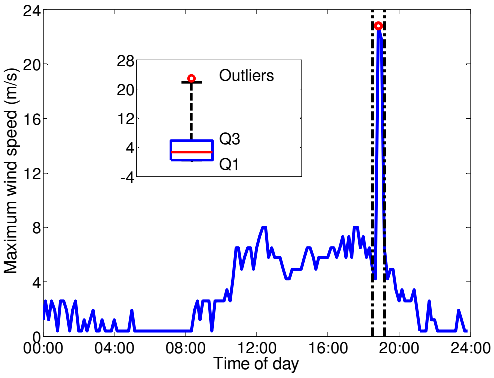

(a) Maximum wind speed

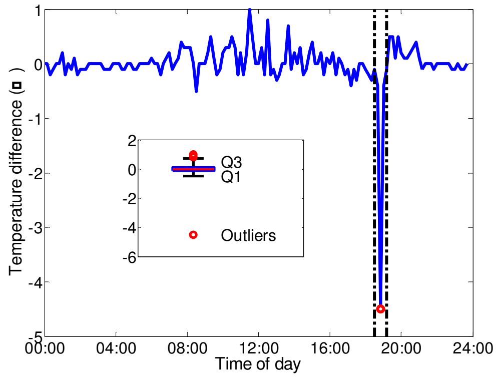

(b) Difference of mean temperature

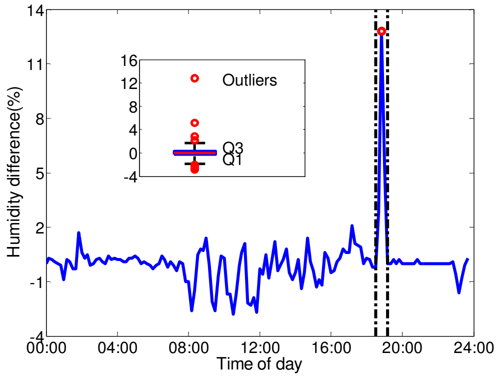

(c) Difference of mean humidity

Fig. 6 Boxplot of parameters for a typical thunderstorm wind (08/08/2014)

Based on the above observations and discussions, an automatic separation algorithm of thunderstorm winds is introduced in detail, as shown in Fig. 8. In the first step, the outlier of the maximum wind speed for the daily wind event will be determined by the boxplot method. If there is no outlier, the wind event will be treated as a non-thunderstorm wind. If some outliers have been detected, the algorithm will run to next step. In the second step, the largest outlier will be compared with a threshold of 15 m/s (Duranona et al. 2006; De Gaetano et al. 2014). Note that this threshold is different from the aforementioned threshold (the mean speed of 8 m/s with 10-min interval), which is used in separating out the 90 most intense (daily) wind events. If it is larger than the threshold, the time of the event is taken to be the 10-min period within which the largest maximum wind speed outlier occurs. For simplicity, this time is referred to as T. In the last step, if the differences of the mean temperature and mean humidity both have outliers within the range of T-20 min and T+20 min, where 20 min is determined as the tolerance, the rapid variation of these parameters should be caused by the same thunderstorm. At this juncture, the wind event will be regarded to be a thunderstorm wind. From these discussions, it can be seen that if there is more than one thunderstorm wind event in one day, the proposed algorithm will only identify the largest one.

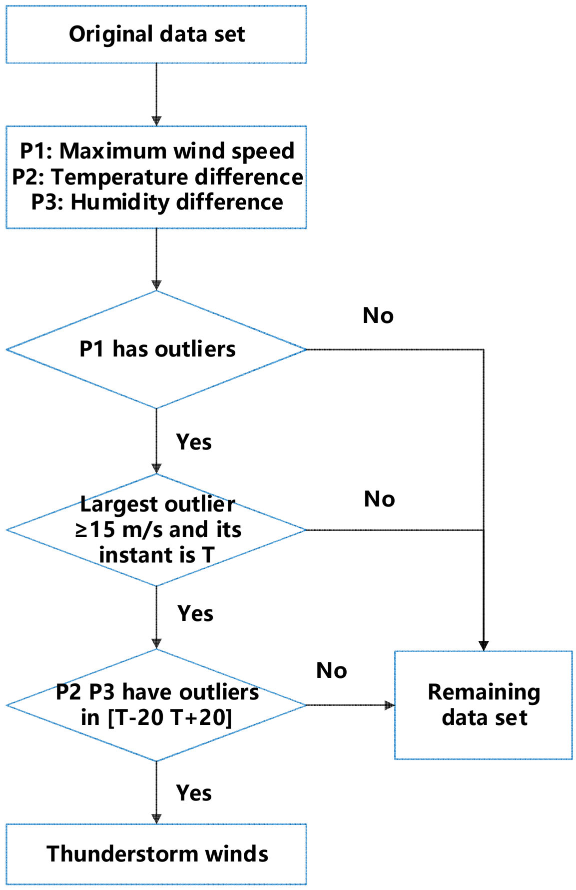

Fig. 7 Automatic separation algorithm of thunderstorm winds

3.2.2 Separation algorithm for thermally developed winds

Due to the close relationship between the mean wind speed and the mean temperature, the thermally developed wind can be determined through the Pearson correlation coefficient r between these two quantities that is defined as their covariance divided by the product of their standard deviations. The variations of the mean wind speed and temperature for different correlation coefficients are shown in Fig. 8. It can be seen that the variation trends of these two quantities tend to coincide when their correlation coefficient is large. For the purpose of this paper it is assumed, as shown in Fig. 8(a) and (b), that a wind event can be treated as a thermally developed one when the above correlation coefficient is greater than 0.4. On the contrary, when the correlation coefficient is less than 0.4, the mean temperature is considered to be not related to the variation of mean wind speed, as shown in Fig. 8(c) and (d). Therefore, such two wind events will not be classified as the thermally developed wind. Based on the above observation, the criterion that the correlation coefficient should be larger than or equal to 0.4 is employed to separate the thermally developed wind.

To alleviate the possible misjudgment due to the use of only the correlation coefficient, the p-value is adopted simultaneously to separate the thermally developed wind. This value is the probability of obtaining a correlation as large as the observed value by random chance, when the true correlation is zero. If the p-value is small, say less than 0.05, the correlation is then significant. Therefore, the p-value which is smaller than or equivalent to 0.05 also serves as a criterion in the separation algorithm of the thermally developed wind. The automatic separation algorithm for the thermally developed wind is shown in Fig. 9. Once the remaining data fail to pass the criterions, the data will be treated as the other wind.

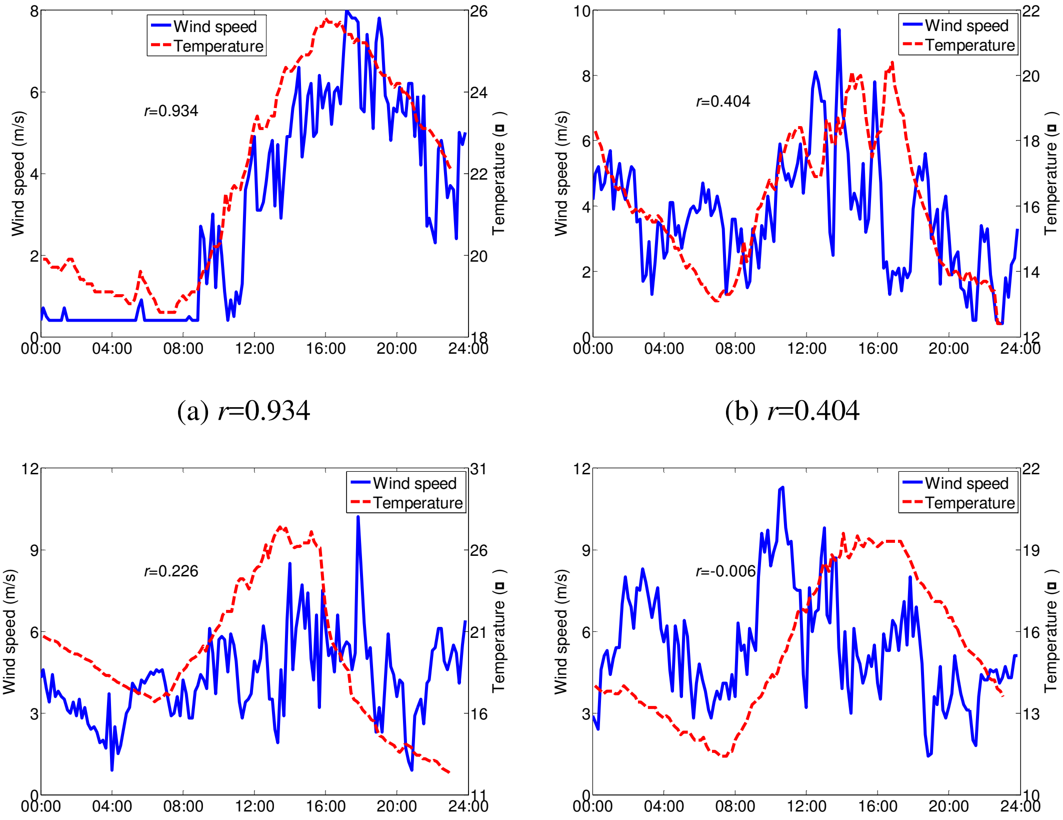

(a) r=0.934 (b) r=0.404

(c) r=0.226 (d) r=-0.006

Fig. 8 Illustration of wind events with different correlation coefficients

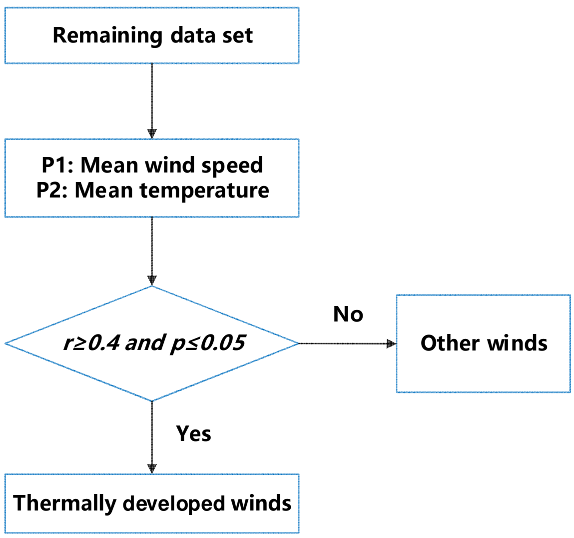

Fig. 9 Automatic separation algorithm of thermally developed winds

3.3 Results and discussion

The results of the above automatic classification method will be given hereafter. In addition, a preliminary discussion about the wind characteristics including the wind speed and direction of all the wind types will be conducted.

3.3.1 Classification results

According to the automatic classification method, 8 thunderstorm wind events have been selected from the 90 most intense (daily) wind events, as shown in Table 2. It reports the maximum wind speed, the gust factor (defined as the ratio of 1-s maximum wind speed to the 10-min mean wind speed), the deviation of the wind direction (defined as the largest difference between the wind directions in a 40-min period centered on the maximum wind velocity instant) and the variation range of the temperature and humidity (defined as the upper and lower bound values in a 40-min period centered on the maximum wind velocity instant). It can be seen that the largest value of the maximum wind speed is 23.8 m/s, and all the gust factors are larger than 1.69. In addition, only two thunderstorm winds have the deviations of wind direction less than 90° and the average deviation of the wind direction for all identified thunderstorm winds is 144°. Finally, the differences between the upper and lower bound values for the temperature and mean humidity are 4.9 °C and 15.7%, respectively. These parameters can provide a reference for identifying thunderstorm winds.

It is worth noting that the maximum thunderstorm wind speeds listed in Table 2 are relatively lower if compared with similar values provided in literature in other countries. This may be due to the relatively short period of measurements and perhaps to the local mountain environment. Further investigations need to be carried out.

Table 2 Summary of measured thunderstorm winds

Date	Maximum wind speed (m/s)	Gust factor	Deviation of Dir. (°)	Range of Temp. (°C)	Range of Humid. (%)
05/07/2013	19.2	1.92	155	[11.6 16.4]	[81.2 96.0]
05/17/2013	19.2	3.84	170	[17.8 21.9]	[76.2 84.0]
06/20/2013	21.8	2.12	145	[16.5 20.6]	[85.9 96.1]
08/02/2013	17.7	1.69	176	[15.4 21.9]	[72.8 96.3]
03/29/2014	16.2	1.69	58	[9.4 14.2]	[78.5 94.7]
08/08/2014	22.8	7.87	179	[18.6 24.0]	[77.0 97.7]
09/10/2014	23.8	2.31	180	[18.8 23.4]	[73.6 96.7]
08/11/2015	16.9	1.86	87	[15.9 21.1]	[87.2 97.1]
Mean	19.7	2.91	144	[15.5 20.4]	[79.1 94.8]

After the extraction of thunderstorm winds, the correlation between the mean wind speed and the mean temperature for the remaining 82-day wind events are examined, as shown in Fig. 10. According to the aforementioned separation algorithm, 62-day thermally developed wind events can be identified. In order to reflect the overall variation feature of the measured thermally developed winds, the normalized mean wind speed, mean temperature and mean humidity are obtained by dividing the daily largest counterparts. Fig. 11 shows the variation of the normalized parameters and wind direction of all the thermally developed winds. It can be seen that the mean wind speed and mean temperature follow a consistent variation trend, and the mean humidity has basically the opposite variation trend. Take the mean wind speed and temperature as an example. They are small at 00: 00-08: 00 and then gradually larger from 08: 00 to 12: 00. Starting from about 12:00, these values increase rapidly and arrive at the peaks at about 16:00. After that, the wind speed and temperature start to decline until midnight. At the duration of 00: 00-08: 00 and 20: 00-24: 00, the wind directions of the majority of days are mainly concentrated in the north, which is in agreement with the direction of down-valley winds. At 08: 00-20: 00, most wind directions are within the range of 200-240 °C, which is in line with the direction of up-valley winds, as shown in Fig. 1. The observed characteristics can to some extent match the statements in literature related to the thermally developed wind (e.g., Whiteman 1990).

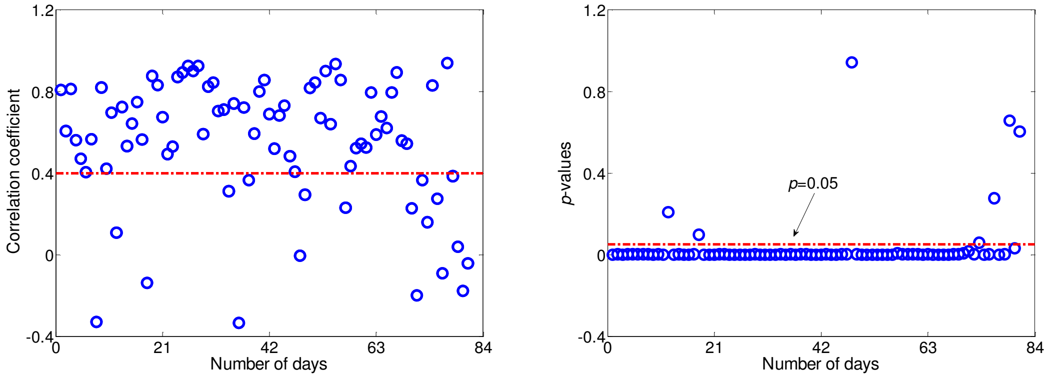

(a) Correlation coefficients (b) *p*-values

Fig. 10 Correlation of all non-thunderstorm wind events

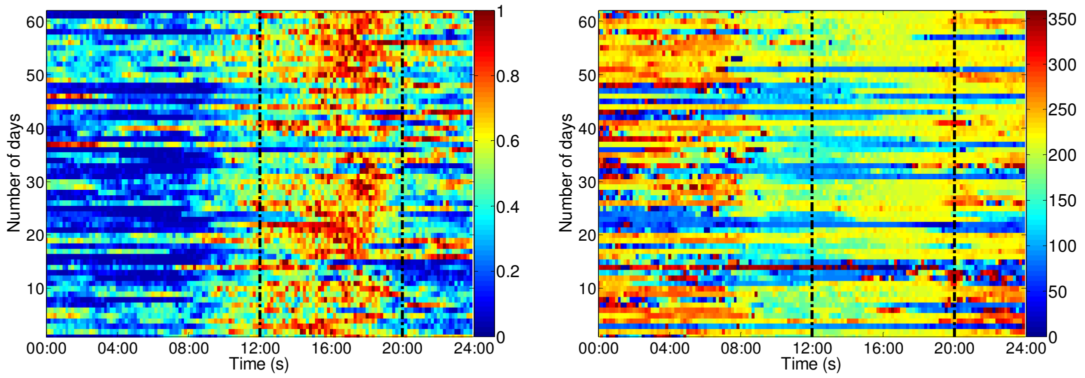

(a) Normalized mean wind speed (b) Mean wind direction

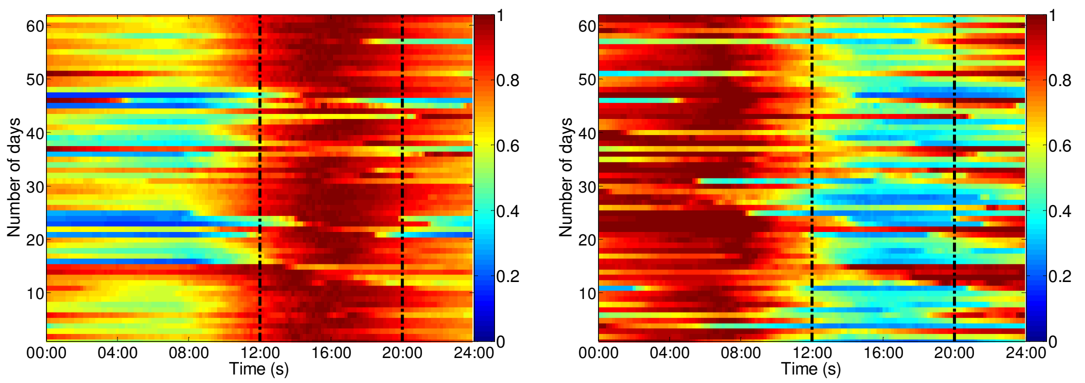

(c) Normalized mean temperature (d) Normalized mean humidity

Fig. 11 Variation trends of all thermally developed winds

In view of the complexity of the wind characteristics in the mountain area, the rest of 20 wind events are regarded as OW. Among the 90 most intense (daily) wind events, there are 8 TWs, 62 TDWs and 20 OWs, which account for 9%, 69% and 22%, respectively. This verifies that TDW is the most frequent wind event in the mountain area. To further investigate the difference of wind types, a preliminary discussion on their wind characteristics including the wind speed and direction will be conducted in the following section.

3.3.2 Preliminary discussion on wind characteristics

For the sake of reasonable comparison, the maximum wind speed instead of the mean wind speed on 10-min interval for all the wind types is analyzed here since the 10-min average value is not representative in the case of the thunderstorm wind due to its rapid variation. The daily largest maximum wind speeds at heights of 10 and 50 m for all the selected intense winds are shown in Fig. 12. It can be observed that the majority of intense winds occurred in February, March and April while the thunderstorm winds always occur from March to September. This is consistent, for instance, with Lombardo et al. (2014). In addition, the average value of the maximum wind speeds of the thunderstorm wind is larger than that of the other wind types, especially for the wind speed at the height of 50 m. This is consistent with the occurrence mechanism of the thunderstorm wind. Finally, the maximum wind speed at the height of 50 m is overall close to that at the height of 10 m. Their largest values are 25.9 and 23.9 m/s for heights of 10 and 50 m, respectively. The winds corresponding to these two values belong to the thermally developed wind and thunderstorm wind, respectively.

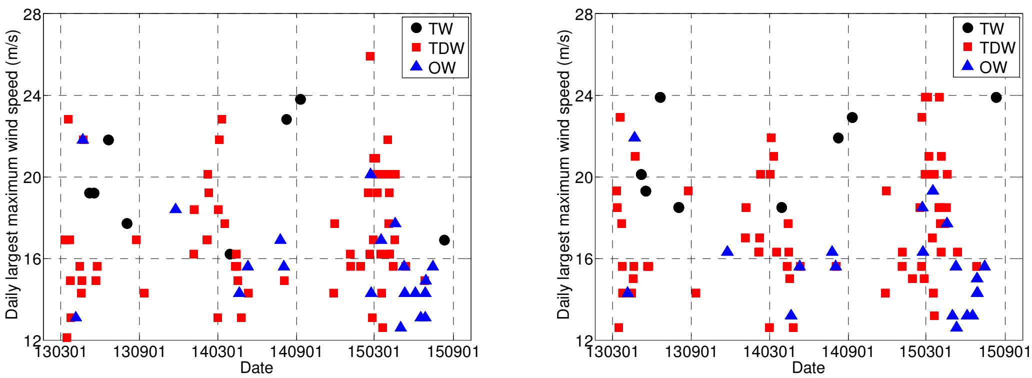

(a) Height of 10 m (b) Height of 50 m

Fig. 12 Daily largest maximum wind speeds for different wind types

The mean wind direction corresponding to the 10-min interval in which the daily largest maximum wind speed occurs is also investigated. The wind roses at 10 m height are shown in Fig. 13. For the thunderstorm wind, the distribution of the wind direction is scattered. The reason may be attributed to the fact that the thunderstorm wind is a mobile small-scale convective event, often embedded in a background flow; so the wind possibly occurs in every direction. The limited representativeness of the mean direction on a 10-min period may strengthen the spread. From Fig. 13(b), it can be seen that the wind directions of the most thermally developed winds are concentrated in the southwest direction, which is mainly due to the influence of valley topography. With reference to the other wind, the overall distribution of the wind direction is also scattered.

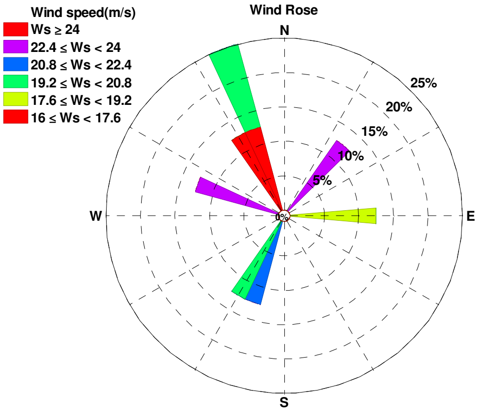

(a) Thunderstorm wind

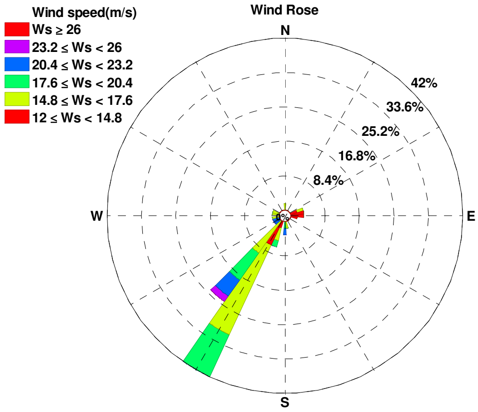

(b) Thermally developed wind

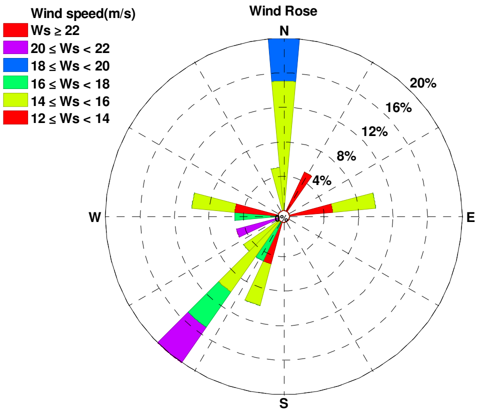

(c) Other wind

Fig. 13 Wind rose of daily largest maximum wind speed (10 m)

Due to the fact that the thunderstorm wind is relatively more important for wind engineering and a broad range of references is available for their analysis, whereas the thermally developed wind deserves some more cautions concerning meteorological aspects and topography features in which they occur, only the wind characteristics of the former will be addressed in the following section. In particular, to better illustrate the thunderstorm fluctuation feature, the 1-hour time history around the maximum wind speed will be chosen from the ultrasonic anemometer data. For the other wind types, further and more specific investigations will be carried out.

4 Wind characteristics of thunderstorm winds

In this section, only the ultrasonic anemometer data are used to analyze the wind characteristics of the thunderstorm wind. For illustration, two typical thunderstorm winds measured on 08/08/2014 and 09/10/2014 are chosen and referred to as Thunderstorm wind 1 and 2, respectively. In the following study, the (vertical) angle of attack (AOA, i.e., the angle between the three-dimensional instantaneous wind velocity and the horizontal plane) will be analyzed firstly. Then, the horizontal wind speed component will be obtained through the decomposition of the data. After the modeling of the horizontal wind speed component, the turbulence intensity and gust factor will be analyzed in detail.

4.1 Angle of attack

The time histories of AOA for the two typical thunderstorm winds are shown in Fig. 14.

To investigate their time-varying means, the moving average method is employed. Since it is difficult to precisely determine the moving average period, a trial is conducted in which the moving average period T1 is set to 100, 200, 300 and 400 s, respectively, as shown in Fig. 14. It can be shown that the time-varying mean at the 400-800 s for Thunderstorm wind 1 deviates from the time-varying trend of the original AOA when T1=400 s is used. For Thunderstorm wind 2, similar case can be found at the 3000-3300 s. When T1=100 s is employed, however, the time-varying mean may include some fluctuations (e.g., 2400-2700 s for Thunderstorm wind 1 and 1900-2200 s for Thunderstorm wind 2). Based on these observations, T1=200 and 300 s seem to be more suitable. At these two cases, the time-varying mean AOAs for these two typical thunderstorm winds both roughly range from 30° to -5°. It should be emphasized that the vertical AOA in a thunderstorm depends on the slope of terrain, the position of the downdraft with respect to the anemometer, the translational speed of the thunderstorm cell, the background flow, and so on. Hence, it is difficult to obtain a generalized feature without a large amount of data.

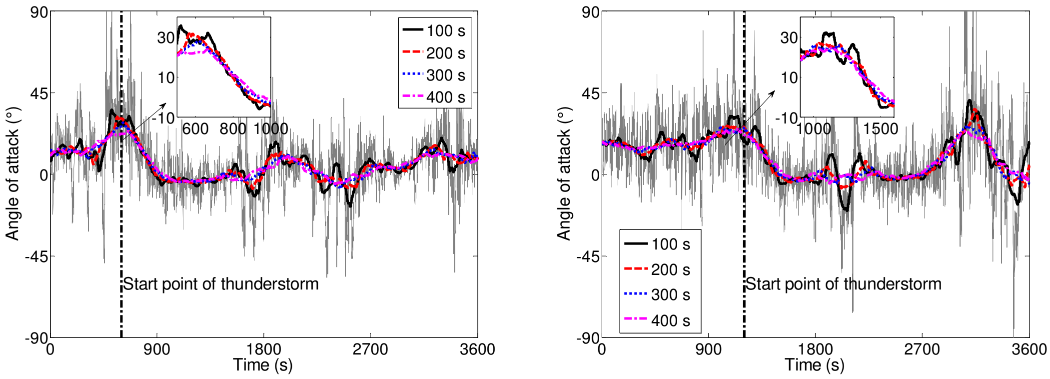

(a) Thunderstorm wind 1 (b) Thunderstorm wind 2

Fig. 14 Time history and time-varying mean of AOA

From the above measurement results, it can be seen that the mean AOA of the thunderstorm wind in the mountain area is overall larger than ±3° in the specification which is determined by the flat area (JTG/T D60-01-2004). This may lead to a larger buffeting response of long-span suspension bridges.

Having defined the AOA, the three-dimensional instantaneous wind speed $\tilde{U}(t)$ can be decomposed as follows

$$U(t) = \tilde{U}(t)\cos(\gamma) \quad (1)$$

where γ is the instantaneous AOA; $U(t)$ is the horizontal wind speed component. Note that only the horizontal wind speed component will be addressed in the following study.

4.2 Modeling of wind speed

The thunderstorm wind can be generally modeled as (Choi and Hidayat, 2002; Chen and Letchford, 2004; Peng et al. 2018)

$$U(t) = \bar{U}(t) + u(t) \quad (2)$$

where $\bar{U}(t)$ is the time-varying mean wind speed; $u(t)$ is the residual turbulence fluctuation.

For the extraction of the time-varying mean wind speed, there are many methods such as the wavelet transform (Wang et al. 2013; Su et al. 2015), empirical model decomposition or ensemble empirical model decomposition (Xu and Chen, 2004; McCullough et al. 2013; Jiang and Huang 2017) and moving average method (Choi and Hidayat, 2002; Solari et al. 2015). In this study, the moving average method is employed for sake of simplicity. Apart from the selection of the method, there is also a wide discussion about how to choose the moving average period. According to different judgment criterions, researchers have suggested different values including 17 or 34 s (Lombardo et al. 2014), 30 s (Riera and Ponte, 2012; Solari et al. 2015; Zhang et al. 2018b), 32 s (Chen and Letchford, 2005; 2006), 60 s (Choi and Hidayat, 2002) and 32 s or 64 s (Su et al. 2015). Based on the above suggestions, 30 s is chosen herein.

The original wind speed and time-varying mean for these two thunderstorm winds are shown in Fig. 15. It can be seen that the time-varying mean can reflect the variation trend of the original wind speed well. In addition, there exist two peak areas for Thunderstorm wind 1 while only one for Thunderstorm wind 2. Following the method proposed in Solari et al. (2015), the thunderstorm duration for these two thunderstorm winds can be calculated, as shown in Fig. 15. They are 297.3 and 202.8 s, respectively. The average value of these two thunderstorm durations is 250.1 s which is very close to 248 s reported in Solari et al. (2015).

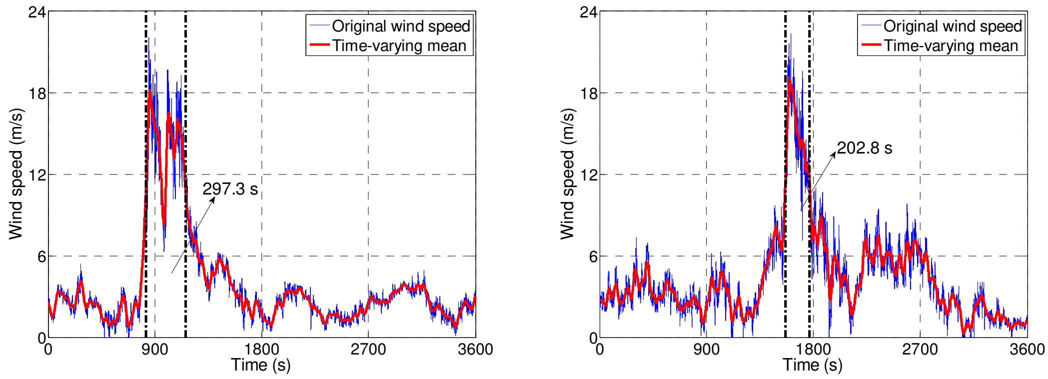

(a) Thunderstorm wind 1 (b) Thunderstorm wind 2

Fig. 15 Modeling of wind speed

After extracting the time-varying mean wind speed, the residual fluctuation of these two thunderstorm winds can be obtained, as shown in Fig. 16. It can be seen that they both show clear nonstationary characteristics. To describe the nonstationarity, the evolutionary power spectral density (EPSD) has been widely used (Priestley, 1965; Chen and Letchford, 2005; Hu and Xu, 2014; Peng et al. 2018). Currently, there are many estimation methods of the EPSD such as the classical Priestley's method (Priestley, 1965), Thomson's multiply window method (Conte and Peng, 1997), wavelet transform-based method (Spanos and Failla, 2004; Huang and Chen, 2009) and so on. For sake of simplicity, the Priestley's method is adopted. The performance of this method is relatively acceptable when only one sample is available while its estimation accuracy requires to be improved when many samples are available. The filter function $g(u)$ and the weight-function $W_{T'}(t)$ in this method are chosen as follows

$$g(u)=\begin{cases}1/(2\sqrt{h\pi}) & |u|\le h\\ 0 & |u|>h\end{cases} \tag{3}$$

$$W_{T'}(t)=\begin{cases}1/T' & |t|\le \frac{1}{2}T'\\ 0 & \text{otherwise}\end{cases} \tag{4}$$

where the parameters are set as $h=7/\Delta t$ and $T'=200/\Delta t$, respectively; and $\Delta t=0.25$ s. The estimated EPSD and its corresponding time-varying standard deviation (STD) are shown in Figs. 17 and 18. For comparison, the moving average method with a window of 30 s is also employed to calculate the time-varying STD, as shown in Fig. 18. It is observed that the maximum spectral values for these two fluctuations appear at around 900 and 1700 s, respectively. In addition, the spectral contents of these two EPSDs are mainly concentrated in the range 0-0.1 Hz. The variation trends of the time-varying STD calculated by the integral through EPSD and moving average method are both consistent with that of the EPSD. Nonetheless, the latter is of larger variation. To further investigate the feature of the EPSD, the normalized EPSD, which is defined as the ratio between EPSD and the time-varying variance, is calculated and shown in Fig. 19. It can be seen that the spectral content at different instants exhibit similar trends, which to some extent verifies the reasonability of simply modeling the nonstationary thunderstorm wind by the uniform modulated random process (Chen and Letchford, 2004; Solari et al. 2015; Huang et al. 2015). Based on this simplified treatment, the reduced turbulence fluctuation, which is defined as the ratio between the residual fluctuation and time-varying STD, can be obtained. The probability density function (PDF) and the statistical moments of the reduced fluctuation are shown in Fig. 20. It can be seen that the skewness of these two reduced fluctuations is nearly zero while the kurtosis is slightly larger than 3.

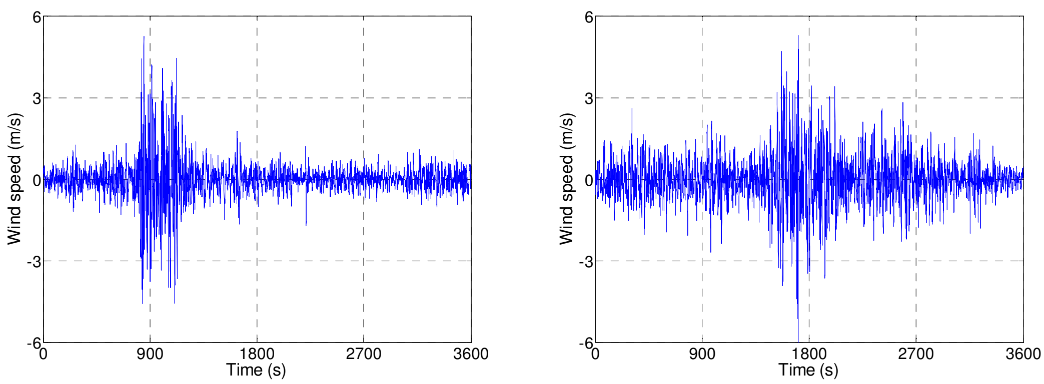

(a) Thunderstorm wind 1 (b) Thunderstorm wind 2

Fig. 16 Residual fluctuations

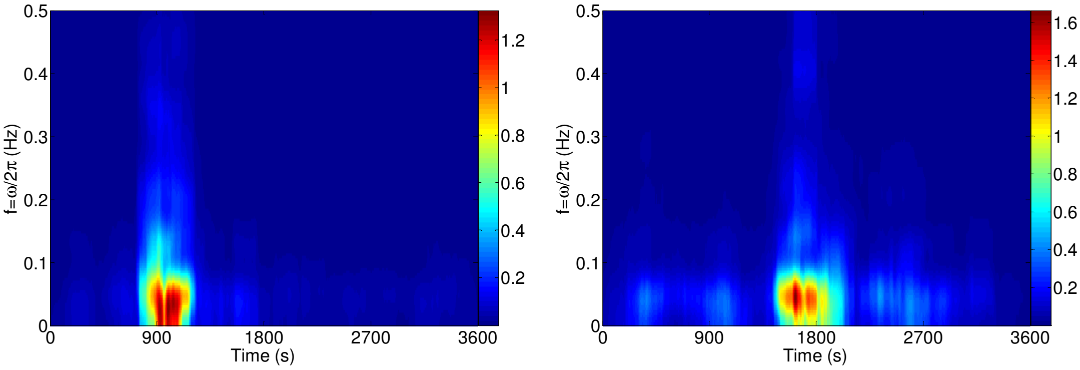

(a) Thunderstorm wind 1 (b) Thunderstorm wind 2

Fig. 17 Estimated EPSDs

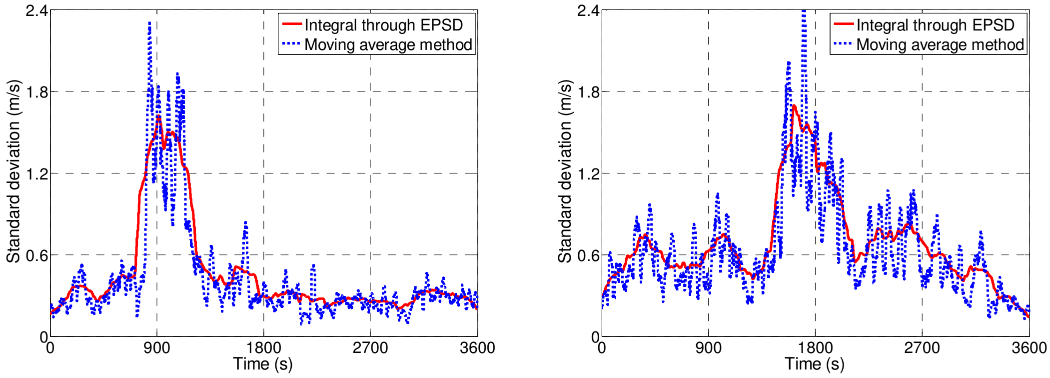

(a) Thunderstorm wind 1 (b) Thunderstorm wind 2

Fig. 18 Time-varying standard deviations

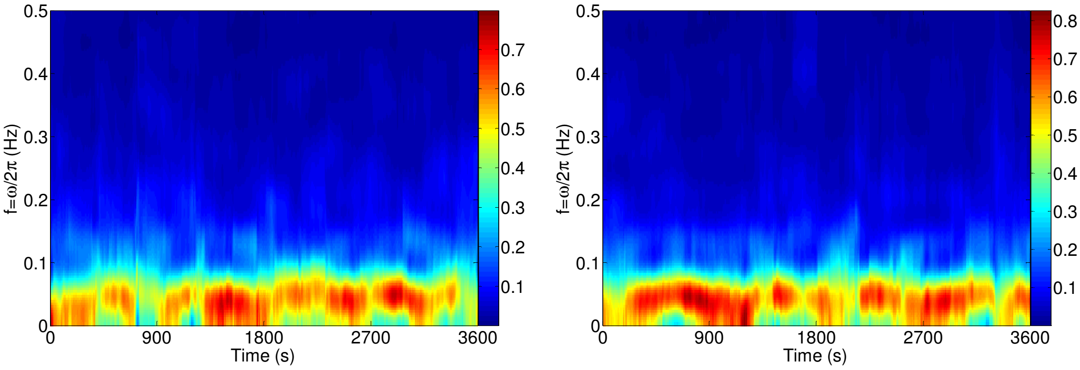

(a) Thunderstorm wind 1 (b) Thunderstorm wind 2

Fig. 19 Normalized EPSDs

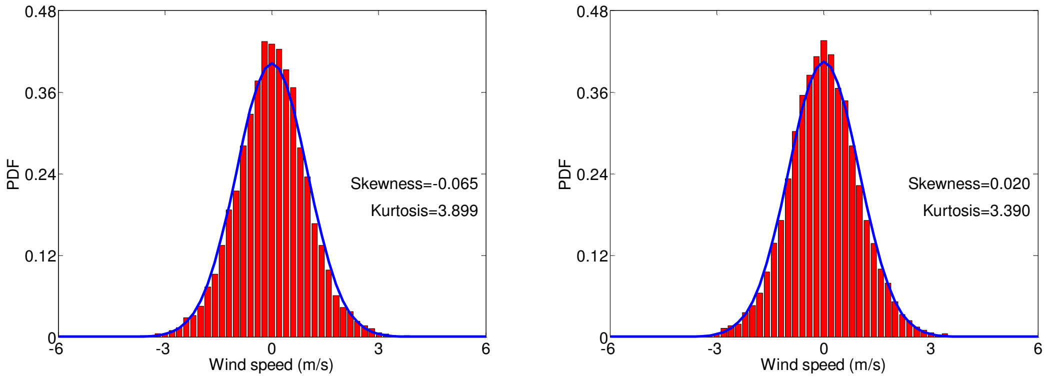

(a) Thunderstorm wind 1 (b) Thunderstorm wind 2

Fig. 20 PDF of the reduced fluctuations

4.3 Turbulence intensity

For the thunderstorm wind, the time-varying turbulence intensity can be expressed as

$$I(t) = \frac{\sigma(t)}{\bar{U}(t)} \tag{5}$$

where $\sigma(t)$ represents the time-varying STD obtained through the integration of the EPSD. Fig. 21 shows the time-varying turbulence intensity for these two thunderstorm winds examined above. It ranges from 0.07 to 0.18 and from 0.07 to 0.13, respectively, in the most intense parts of the records. The average values of these two quantities are both 0.10, which is close to the values 0.085-0.088, 0.09-0.11 and 0.12 measured in the flat area (Chen and Letchford, 2004; Holmes et al. 2008; Solari et al. 2015; Zhang et al. 2018b).

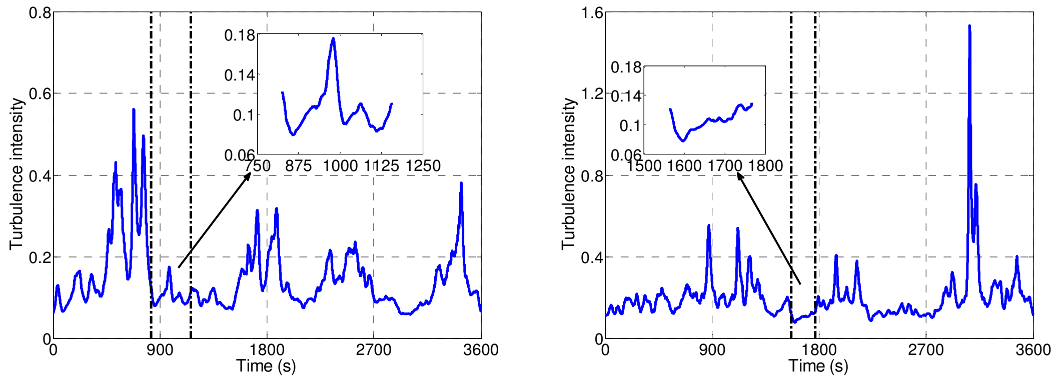

(a) Thunderstorm wind 1 (b) Thunderstorm wind 2

Fig. 21 Time-varying turbulence intensities

4.4 Gust factor

As emphasized in literature, there are many definitions of gust factors for thunderstorm winds, which may lead to different results (Solari et al. 2015; Lombardo et al. 2014). In this study, the gust factor of the thunderstorm wind G_t is defined as (Holmes et al. 2008; Chay et al. 2008; Lombardo et al. 2014)

$$G_t = \bar{U}_t / \bar{U}_{\max}(t) \tag{6}$$

where $\bar{U}_t$ is the largest value of the running average wind speed over $t = 1$ s; $\bar{U}_{\max}(t)$ is the largest value of the time-varying mean wind speed. The gust factors of the aforementioned two typical thunderstorm winds are 1.18 and 1.14, respectively. These values are close to 1.25 and 1.2 measured in the flat area (Holmes et al. 2008; Solari et al. 2015).

5 Summary and conclusions

This paper addressed the intense wind characteristics in mountain area based on the field measurement. Through the examination of the data measured by the cup anemometer, two typical wind events in the mountain area, the thunderstorm wind and thermally developed wind, were highlighted. To separate these wind events, an automatic classification method was proposed, which includes the separation algorithms for thunderstorm winds and thermally developed winds. The former utilizes the boxplot method to capture the rapid variation of the maximum wind speed, mean temperature and humidity of the thunderstorm wind while the latter relies on the correlation between the mean wind speed and temperature. The extraction and classification results of all the wind types and the preliminary discussion on their wind characteristics were provided, which illustrate the effectiveness of the proposed classification method. However, only the characteristics of the thunderstorm wind were analyzed in detail based on the ultrasonic anemometer data. Results are summarized as follows:

1) The maximum wind speeds discussed in this paper are relatively lower when compared with values provided by literature in other countries. This may be in part due to the short period of measurements and perhaps to the local mountain environment. Further investigations are needed.

2) The majority of intense winds occurred in February, March and April while the thunderstorm winds always occur from March to September. The distribution of wind directions for the thunderstorm wind is scattered while the wind directions of the most thermally developed winds are concentrated in the southwest direction.

3) The time-varying mean (vertical) angle of attack of the two typical thunderstorm winds ranges from around 30° to -5° around the time at which thunderstorm winds are most intense.

4) The durations for the two typical thunderstorm winds are 297.3 and 202.8 s, respectively. Their average value, 250.1 s, is very close to the measurement in the flat area.

5) The spectral values of the normalized EPSDs at different instants exhibit similar variation trends. This to some extent verifies the reasonability of simply modeling the nonstationary thunderstorm winds by the uniformly modulated random process.

6) The average value of the time-varying turbulence intensity in correspondence of the most intense part of the thunderstorm wind is 0.10, which is close to that measured in the flat area. The gust factors of the two typical thunderstorm winds are 1.18 and 1.14, which are close to the values reported in the flat area.

Due to the limited data in this study, further investigations on the characteristics of the intense mountain wind should be conducted, especially by the field measurement.

6 Acknowledgements

The support by the National Natural Science Foundation of China (Grant Nos. 51720105005, 51578471, 51808078) are greatly acknowledged. This research is also supported by the China Postdoctoral Science Foundation (Grant No. 2018M640900), 111

Project (Grant No. B18062) and the Chinese Fundamental Research Funds for the Central Universities (Grant No. 2018CDXYTM0003). The fourth author acknowledges the support by European Research Council under the European Union's Horizon 2020 research and innovation program for the project THUNDERR- Detection, simulation, modelling and loading of thunderstorm outflows to design wind-safer and cost-efficient structures (Grant No. 741273).

Appendix A

The boxplot method can graphically depict groups of the data through their quartiles (Tukey, 1977). There are many calculation methods of quartiles. In this study, the following method is selected. Consider an original ordered data set $X=[X(1),X(2),\cdots,X(m)]$. The calculation formulas of the first quartile (Q1) and third quartile (Q3) are shown in Table 4, where n is a positive integer. The interquartile range (IQR) is defined as Q3 minus Q1. Subsequently, the outlier P is defined as follows

$$\mathrm{P}<\mathrm{Q1}-3.0\times\mathrm{IQR} \text{ or } \mathrm{P}>\mathrm{Q3}+3.0\times\mathrm{IQR} \tag{7}$$

Coming to the plot, the lower and upper boundaries of the box represent the first and third quartiles, respectively. The ends of the whiskers represent the minimum and maximum of all of the data. Any data not included between the whiskers will be plotted as an outlier with red circle.

Although this method lacks of theoretical background, experience shows that it performs well in dealing with the actual data. In comparison with the traditional method such as the 3σ method, the boxplot method has two advantages. First, the assumption of *a prior* distribution of the data is not required. Second, the results of the identification of outliers are robust. This is attributed to the fact that up to 25% of the data can be arbitrarily distant without greatly disturbing the quartiles and the relative identification criterion of outliers (McGill et al. 1978).

Table 4 Calculation formulas of quartiles

	First quartile (Q1)	Third quartile (Q3)
$m=4n$	$0.5[X(n)+X(n+1)]$	$0.5[X(3n)+X(3n+1)]$
$m=4n+1$	$0.25X(n)+0.75X(n+1)$	$0.75X(3n+1)+0.25X(3n+2)$
$m=4n+2$	$X(n+1)$	$X(3n+2)$
$m=4n+3$	$0.75X(n+1)+0.25X(n+2)$	$0.25X(3n+2)+0.75X(3n+3)$

7 References

Berg, J., Mann, J., Bechmann, A., Courtney, M. S., and Jørgensen, H. E. (2011). "The bolund experiment, Part I: flow over a steep, three-dimensional hill." Boundary-Layer Meteorology, 141(2), 219-243.

Burlando, M., De Gaetano, P., Pizzo, M., Repetto, M. P., Solari, G., and Tizzi, M. (2013). "Wind climate analysis in complex terrain." Journal of Wind Engineering and Industrial Aerodynamics, 123, 349-362.

Burlando, M., Tizzi, M., and Solari, G. (2017a). "Characteristics of downslope winds in the Liguria region." Wind and Structures, An International Journal, 24(6), 613-635.

Burlando, M., Romanic, D., Solari, G., Hangan, H., and Zhang, S. (2017b). "Field data analysis and weather scenario of a downburst event in Livorno, Italy on 1 October 2012." Monthly Weather Review, 145(9), 3507-3527.

Conte, J. P., and Peng, B. F. (1997). "Fully non-stationary analytical earthquake ground-motion model." Journal of Engineering Mechanics, 123(1), 15-24.

Choi, E. C. C. and Hidayat, F. A. (2002). "Dynamic response of structures to thunderstorm winds." Progress in Structural Engineering and Materials, 4, 408-416.

Choi, E. C. C., and Tanurdjaja, A. (2002). "Extreme wind studies in Singapore. An area with mixed weathersystem." Journal of Wind Engineering and Industrial Aerodynamics, 90, 1611-1630.

Castino, F., Rusca, L., and Solari, G. (2003). "Wind climate micro-zoning: A pilot application to Liguria Region (North-Western Italy)." Journal of Wind Engineering and Industrial Aerodynamics, 91, 1353-1375.

Cook, N. J., Harris, R. I., and Whiting, R. (2003). "Extreme wind speeds in mixed climates revisited." Journal of Wind Engineering and Industrial Aerodynamics, 91, 403-422.

Choi, E. C. C. (2004). "Field measurement and experimental study of wind speed profile during thunderstorms." Journal of Wind Engineering and Industrial Aerodynamics, 92(3-4), 275-290.

CCCC Highway Consultants CO., Ltd. (2004). "Wind-resistent design specification for highway bridges." JTG/T D60-01-2004, Standard Press of China, Beijing. (In Chinese)

Chock, G. Y. K., and Cochran, L. (2005). "Modeling of topographic wind speed effects in Hawaii." Journal of Wind Engineering and Industrial Aerodynamics, 93 (8), 623-638.

Chen, L., and Letchford, C. W. (2004). "A deterministic-stochastic hybrid model of downbursts and its impact on a cantilevered structure." Engineering Structures, 26(5), 619-629.

Chen, L., and Letchford, C. W. (2005). "Proper orthogonal decomposition of two vertical profiles of full-scale nonstationary downburst wind speeds." Journal of Wind Engineering and Industrial aerodynamics, 93(3), 187-216.

Chen, L., and Letchford, C. W. (2006). "Multi-scale correlation analyses of two lateral profiles of full-scale downburst wind speeds." Journal of Wind Engineering and Industrial Aerodynamics, 94(9), 675-696.

Carrera, M. L., Gyakum, J. R., and Lin, C. A. (2009). "Observational study of wind channeling within the St. Lawrence River Valley." Journal of Applied Meteorology and Climatology, 2009, 48(11), 2341-2361.

Cao, S., Wang, T., Ge, Y., and Tamura, Y. (2012). "Numerical study on turbulent boundary layers over two-dimensional hills -Effects of surface roughness and slope." Journal of Wind Engineering and Industrial Aerodynamics, 104, 342-349.

Chow, F. K., Wekker, S. F. J. D., and Snyder, B. J. (2013). "Mountain Weather Research and Forecasting." Springer Netherlands.

Cantelli, A., Monti, P., Leuzzi, G., Valerio, G., and Pilotti, M. (2017). "Numerical simulations of mountain winds in an alpine valley." Wind and Structures, An International Journal, 24(6), 565-578.

Defant, F. (1951). "Local winds. Compendium of meteorology." American Meteorological Society, Boston, Massachusetts, 655-672.

Durañona, V., Sterling, M., and Baker, C. J. (2007). "An analysis of extreme non-synoptic winds." Journal of Wind Engineering and Industrial Aerodynamics, 95(9-11), 1007-1027.

Davidson, B. (2010). "Some turbulence and wind variability observations in the lee of mountain ridges." Journal of applied meteorology, 2(4), 463-472.

De Gaetano, P., Repetto, M. P., Repetto, T., and Solari, G. (2014). "Separation and classification of extreme wind events from anemometric records." Journal of Wind Engineering and Industrial Aerodynamics, 126, 132-143.

Fenerci, A., Øiseth, O., and Rønnquist, A. (2017). "Long-term monitoring of wind field characteristics and dynamic response of a long-span suspension bridge in complex terrain." Engineering Structures, 147, 269-84.

Fenerci, A., and Øiseth, O. (2018). "Strong wind characteristics and dynamic response of a long-span suspension bridge during a storm." Journal of Wind Engineering and Industrial Aerodynamics, 172, 116-138.

Gomes, L., and Vickery, B. J., (1977/1978). "Extreme wind speeds in mixed climates." Journal of Wind Engineering and Industrial Aerodynamics, 2, 331-344.

Gunter, W. S., and Schroeder, J. L. (2013). "High-resolution full-scale measurements of thunderstorm outflow winds." In: Proceedings of the 12th Americas Conference on Wind Engineering. Seattle, Washington.

Hunt, J. C. R., Leibovich, S., and Richards, K. J. (1988). "Turbulent shear flow over hills." Quarterly Journal of the Royal Meteorological Society, 114(484), 1435-1470.

Holmes, J. D., Hangan, H. M., Schroeder, J. L., Letchford, C. W., and Orwig, K. D. (2008). "A forensic study of the Lubbock-Reese downdraft of 2002." Wind and Structures, An International Journal, 11, 19-39.

Huang, G., and Chen, X. (2009). "Wavelets-based estimation of multivariate evolutionary spectral and its application to nonstationary downburst winds." Engineering Structures, 31(4), 976-989.

Hu, L. and Xu, Y. L. (2014). "Extreme value of typhoon-induced non-stationary buffeting response of long-span bridges." Probabilistic Engineering Mechanics, 36, 19-27.

Huang, G., Zheng, H., Xu, Y. L., and Li, Y. (2015). "Spectrum models for nonstationary extreme winds." Journal of Structural Engineering, ASCE, 141(10): 04015010.

Huang, G., Peng, L., Su, Y., Liao, H. and Li, M. (2015). "A wireless high-frequency anemometer instrumentation system in field measurement." Wind and Structures, An International Journal, 20(6), 739-749.

Huang, G., Cheng, X., Peng, L., and Li, M. (2018). "Aerodynamic shape of transition curve for truncated mountain terrain model in wind field simulation." Journal of Wind Engineering and Industrial Aerodynamics, 178, 80-90.

Jackson, P. S., and Hunt, J. C. R. (1975). "Turbulent wind flow over a low hill." Quarterly Journal of the Royal Meteorological Society, 101(430), 929-955.

Jackson, P. L., Mayr, G., and Vosper, S. (2013). "Dynamically-Driven Winds." Mountain Weather Research and Forecasting. Springer Netherlands.

Jiang, Y., and Huang, G. (2017). "Short-term wind speed prediction: hybrid of ensemble empirical mode decomposition, feature selection and error correction." Energy Conversion and Management, 144, 340-350.

Kasperski, M. (2002). “A new wind zone map of germany.” Journal of Wind Engineering and Industrial Aerodynamics, 90(11), 1271-1287.

Lombardo, F. T., Main, J. A., and Simiu, E. (2009). “Automated extraction and classification of thunderstorm and non-thunderstorm wind data for extreme-value analysis.” Journal of Wind Engineering and Industrial Aerodynamics, 97(3), 120-131.

Li., C. G., Chen., Z. Q., Zhang., Z. T., and Cheung., J. C. K. (2010). “Wind tunnel modeling of flow over mountain valley terrain.” Wind & Structures An International Journal, 13(3), 275-295.

Lombardo, F. T., Smith, D. A., Schroeder, J. L. and Mehta, K. C. (2014). “Thunderstorm characteristics of importance to wind engineering.” Journal of Wind Engineering and Industrial Aerodynamics, 125, 121-132.

Li, Y., Hu, P., Xu, X., and Qiu, J. (2017). “Wind characteristics at bridge site in a deep-cutting gorge by wind tunnel test.” Journal of Wind Engineering and Industrial Aerodynamics, 160, 30-46.

McGill, R., J. W. Tukey, and W. A. Larsen. (1978). “Variations of Boxplots.” The American Statistician. 32(1), 12-16.

Mitsuta, Y., Tsukamoto, O., and Nenoi, M. (1983). “Wind characteristics over complex terrain.” Journal of Wind Engineering and Industrial Aerodynamics, 15(15), 185-196.

Momomura, Y., Marukawa, H., Okamura, T., Hongo, E., and Ohkuma, T. (1997). “Full-scale measurements of wind-induced vibration of a transmission line system in a mountain area.” Journal of Wind Engineering and Industrial Aerodynamics, 72(1), 241-252.

Masters, F. J., Vickery, P. J., Bacon, P., and Rappaport, E. N. (2010). “Toward objective, standardized intensity estimates from surface wind speed observations.” Bulletin of the American Meteorological Society, 91(12), 1665-1681.

McCullough, M., Kwon, D. K., Kareem, A., and Wang, L. (2013). “Efficacy of averaging interval for non-stationary winds.” Journal of Engineering Mechanics, 140(1), 1-19.

Okamura, T., Ohkuma, T., Hongo, E., and Okada, H. (2003). “Wind response analysis of a transmission tower in a mountain area.” Journal of Wind Engineering and Industrial Aerodynamics, 91(1), 53-63.

Priestley, M. B. (1965). “Evolutionary spectra and non-stationary processes.” Journal of the Royal Statistical Society. Series B (Methodological), 27(2), 204-237.

Peng, L., Huang, G., Chen, X., and Yang, Q. (2018). “Evolutionary spectra-based time-varying coherence function and application in structural response analysis to downburst winds.” Journal of Structural Engineering, 144(7), 04018078.

Riera, J. D., and Nanni, L. F. (1989). “Pilot study of extreme wind velocities in a mixed climate considering wind orientation.” Journal of Wind Engineering and Industrial Aerodynamics, 32(1-2), 11-20.

Riera, J. D., and Ponte, J. (2012). “Recent brazilian research on thunderstorm winds and their effects on structural design.” Wind and Structures, An International Journal, 15(15), 111-129.

Taylor, P. A., and Teunissen, H. W. (1987). “The Askervein hill project: overview and background data.” Boundary-Layer Meteorology, 39(1-2), 15-39.

Salmon, J. R., Bowen, A. J., Hoff, A. M., Johnson, R., Mickle, R. E., and Taylor, P. A., Tetzlaff, G., and Walmsley, J. L. (1988). "The Askervein hill project: mean wind variations at fixed heights above ground." Boundary-Layer Meteorology, 43(3), 247-271.

Spanos, P. D., and Failla, G. (2004). "Evolutionary spectral estimation using wavelets." Journal of Engineering Mechanics, 130(8), 952-960.

Shu, Z. R., Li, Q. S., He, Y. C., and Chan, P. W. (2015). "Gust factors for tropical cyclone, monsoon and thunderstorm winds." Journal of Wind Engineering and Industrial Aerodynamics, 142, 1-14.

Solari, G., Burlando, M., De Gaetano, P., and Repetto, M. P. (2015). "Characteristics of thunderstorms relevant to the wind loading of structures." Wind and Structures, An International Journal, 20, 763-791.

Su, Y. W., Huang, G. Q., and Xu, L. (2015). "Derivation of time-varying mean for non-stationary downburst winds." Journal of Wind Engineering and Industrial Aerodynamics, 141, 39-48.

Tukey, J. W., (1977). "Exploratory Data Analysis." Addison-Wesley, Reading, Massachusetts, 39-49.

Whiteman, C. D. (1990). "Observations of thermally developed wind systems in mountain terrain. Chapter 2 in Atmospheric Processes over Complex Terrain." Meteorological Monographs, American Meteorological Society, Boston, Massachusetts, 5-42.

Wang, L., McCullough, M., and Kareem, A. (2013). "A data-driven approach for simulation of full-scale downburst wind speeds." Journal of Wind Engineering and Industrial aerodynamics, 123, 171-90.

Xu, Y. L., and Chen, J. (2004). "Characterizing nonstationary wind speed using empirical mode decomposition. Journal of Structural Engineering, 130(6), 912-920.

Zhu, L., Ren, P., Chen, W., Zhou, Q., and Wang, J. (2011). "Investigation on wind profiles in the deep gorge at the Balinghe bridge site via field measurement. Journal of Experiments in Fluid Mechanics, 25(4), 15-21. (In Chinese)

Zhang, S., Solari, G., De Gaetano, P., Burlando, M., and Repetto, M. P. (2018). "A refined analysis of thunderstorm outflow characteristics relevant to the wind loading of structures." Probabilistic Engineering Mechanics, 54, 9-24.

Zhang, S., Solari, G., Yang, Q., and Repetto, M. P. (2018). "Extreme wind speed distribution in a mixed wind climate." Journal of Wind Engineering and Industrial Aerodynamics, 176, 239-253.